HOKKAIDO UNIVERSITY

Title	Key biogeochemical processes evaluated by the stable nitrogen isotopes of dissolved inorganic nitrogen in the Yodo River estuary, Japan: significance of estuarine nutrient recycling as a possible source for coastal production
Author(s)	Sugimoto, Ryo; Kasai, Akihide
Citation	Biogeochemistry, 128(1-2), 1-17 https://doi.org/10.1007/s10533-016-0190-z
Issue Date	2016-03
Doc URL	http://hdl.handle.net/2115/64622
Rights	The final publication is available at link.springer.com
Rights(URL)	http://creativecommons.org/licenses/by-nc-nd/4.0/
Type	article (author version)
File Information	Kasai Revision 3-1.pdf

Instructions for use

Hokkaido University Collection of Scholarly and Academic Papers : HUSCAP

Key biogeochemical processes evaluated by the stable nitrogen isotopes of dissolved inorganic nitrogen in the Yodo River estuary, Japan: Significance of estuarine nutrient recycling as a possible source for coastal production

Ryo Sugimoto[1*], Akihide Kasai[2]

(1) Research Center for Marine Bioresources, Fukui Prefectural University, 49-8-2 Katsumi, Obama, Fukui 917-0116, Japan
(2) Field Science Education and Research Center, Kyoto University, Oiwake, Kitashirakawa, Sakyo, Kyoto, 606-8502, Japan

Present address: A. Kasai

Faculty of Fisheries Sciences, Hokkaido University, 3-1-1, Minato-cho, Hakodate, Hokkaido 041-8611, Japan

* Corresponding author: R. Sugimoto
Tel: +81-770-52-7305
Fax: +81-770-52-7306
E-mail: sugiryo@fpu.ac.jp

Abstract

Isotope analysis of dissolved inorganic nitrogen (DIN) and a mixing model along the salinity gradient were used to clarify the dominant biogeochemical processes controlling nutrient dynamics within a shallow eutrophic estuary in Japan. Although delivery of riverine DIN into the estuary is largely dominated by mixing with seawater during most months, internal biogeochemical processes of DIN assimilation by phytoplankton and DIN production by remineralization and subsequent nitrification within the estuary offer the most reasonable explanation for observed deviations in the isotopic compositions of NO_3^- from mixing behavior. However, the balance of each process changed over time. During phytoplankton blooming in summer, co-occurrence of NO_3^- assimilation and NO_3^- regeneration inhibited the accumulation of NO_3^- within the estuary. Moreover, assimilation of NH_4^+ as well as NO_3^- by phytoplankton complicates the nutrient dynamics within the estuary. However, mostly conservative or productive behavior of DIN as well as PO_4^{3-} showed that recycled nutrients are significant net source within the estuary. These results suggest recycled nutrients within the estuary could have a non-negligible impact on eutrophication in Osaka Bay.

Keywords

Nutrient, Stable isotope, Eutrophication, Regeneration, Estuary

1. Introduction

Estuaries have an important role in regulating nutrient fluxes from land to sea. The estuaries of major rivers are considered as active sites for reducing riverine nitrogen loads to coastal seas (Brion et al. 2004; Seitzinger et al. 2006). However, several studies suggest that estuarine removal of reactive nitrogen may be significantly overrated (Jickells et al. 2000; Tobias et al. 2003). Several recent studies showed that estuaries may be a significant source of nitrogen to coastal systems (Dänke et al. 2008; Xue et al. 2014). Therefore, global concerns about the nutrient enrichment of estuaries have directed considerable focus toward understanding how nutrients are transported and transformed at the land–sea interface.

A variety of biogeochemical processes distributes nutrients between inorganic and organic forms, and between the pelagic and benthic compartments of estuaries. To clarify the roles of biogeochemical processes such as denitrification, nitrification, and primary production, rate measurements of each process at a variety of spatial and temporal scales are effective (Thompson 1998; Ragueneau et al. 2002; Giblin et al. 2010; Roberts et al. 2012). However, a large number of rate measurements are needed to describe the system thoroughly, which requires considerable technical expertise and intense research efforts.

A mixing diagram of concentration data against salinity provides a convenient method to display the net result of nutrient transformations in an estuary and gives an indication of likely occurring biogeochemical processes (Eyre 2000). However, it is not possible to determine whether conservative behavior is due to a lack of activity or to an approximate balance between production and consumption. Additional measurements of stable nitrogen isotopes ($\delta^{15}N$) of dissolved inorganic nitrogen (DIN) provide an effective method to assess the internal turnover processes of nitrogen and sources in estuaries (Middelburg and Nieuwenhuize 2001). The ability to detect small differences in the ^{15}N:^{14}N ratio of various pools of nitrogen, combined with knowledge of kinetic isotope fractionation in chemical and biological reactions, potentially provides ways to monitor nitrogen transformations on various temporal and spatial scales (Sugimoto et al. 2010; 2014). For instance, denitrification leaves behind NO_3^- enriched in ^{15}N, whereas nitrification results in the formation of ^{15}N depleted NO_3^- relative to the original NH_4^+ pool. The combined use of nutrient concentrations and $\delta^{15}N$ values of DIN makes it possible to determine whether observed concentrations represent conservative or balance between sources and sinks.

This study was conducted in the estuarine zone of the Yodo River, which empties into Osaka Bay (Fig. 1). Osaka Bay is one of the most eutrophic coastal areas in Japan (Tsujimoto et al. 2006; Yashuhara et al. 2007). Whereas efforts have been made to reduce nutrient loads from the rivers in the last few decades (Nakatani et al. 2011), riverine nutrient discharge is thought to have significant effects on the formation of hypoxic or anoxic conditions in the bottom water at the head of the bay during summer (Nakajima and Fujiwara 2007), and red tides often occur throughout the year in the bay (Hayashi and Yanagi 2008). In recent years, a harmful algal bloom (HAB) of *Alexandrium tamarense* has been observed at the head of the bay (Yamamoto et al. 2009). Although the intrusion of saltwater into the estuary is well documented (Yamamoto et al. 2013), there is little knowledge about estuarine nutrient dynamics.

The goal of this study was to account for DIN behavior within the Yodo River estuary and to assess DIN losses in the estuary to better constrain the effect of riverine nutrients on eutrophication in Osaka Bay. Therefore, we examined the concentrations and $\delta^{15}N$ values of NO_3^- and NH_4^+, as well as other parameters such as phosphorus and chlorophyll-*a* (Chl-*a*) concentrations to clarify how the dominant biogeochemical processes affect nutrient dynamics within the eutrophic Yodo River estuary.

2. Materials and methods

2.1. Study site

The Yodo River is the largest river flowing into Osaka Bay (Fig. 1). It drains a catchment area of 8240 km^2, which contains a population of approximately 11 million. Large amounts of nutrients are released into the inner part of the bay through the Yodo River, causing significant eutrophication in the region. The estuarine zone in the Yodo River is shallow and shortened by a weir located 15 km upstream from the river mouth (Fig. 1). The weir is used for flood control and ensures that enough water is available for various upstream uses. During low precipitation and/or low freshwater discharge periods, seawater extends up to the weir (Yamamoto et al. 2013).

Nutrient concentrations in the river are monitored by the Ministry of Land, Infrastructure and Transport (MLIT), Japan (http://www1.river.go.jp/) (a triangle in Fig. 2). Riverine nitrogen is composed mainly of DIN (76% on average), although the proportion changes seasonally, becoming lower in summer (June to July) and higher in winter (December to January). NO_3^- is the dominant form of DIN. Proportions of NH_4^+ in DIN are less than 10%. Although dissolved inorganic phosphorus (DIP) concentrations change from 0.4 to 2.9 μM, the DIN/DIP (N/P) ratios are always higher than the Redfield ratio of 16 (Redfield et al. 1963).

2.2. Field sampling

Transect surveys from the bay head of Osaka Bay to the lower part of the Yodo River (circles in Fig. 1) were conducted during the spring tide in each season: spring (30 May 2010 and 17 May 2011), summer (15 July 2011), autumn (8 November 2011) and winter (21 February 2012). The observations were started from the offshore station (Stn. Y10) to the upper estuarine station (Stn. Y5) during the morning ebb tide. At each station, water temperature, salinity, and dissolved oxygen (DO) concentration were measured vertically by a CTD (JFE Advantech, ASTD102).

Water samples (5L) for chemical analysis were collected vertically from the surface to bottom layers (three to five layers; Tables 1 to 5) at each station using a 6-L Van Dorn Water Sampler (RIGO, Horizontal type).

In the laboratory, 100 mL water was filtered through precombusted (450°C, 3 h) glass fiber filters (25 mm diameter, Whatman GF/F). The filters were soaked separately in 5 mL *N*,*N*-dimethylformamide (DMF) in polypropylene tubes and stored in the dark at 4°C for subsequent Chl-*a* analysis. Other water samples were filtered through precombusted glass fiber filters (25 or 47 mm diameter and 0.7 μm pore size, Whatman GF/F), and the filters were stored individually in glass vials at -30°C until later analysis for nitrogen and carbon isotopes of particulate organic matter (POM). Filtrate was stored separately at -30°C for later analyses of concentration and $\delta^{15}N$ of NO_3^- and NH_4^+.

2.2. Chemical analyses

The Chl-*a* concentration in the bulk POM on GF/F was quantified using a calibrated fluorometer (Trilogy, Turner Design). The NO_3^-, NO_2^-, and PO_4^{3-} concentrations were measured using an autoanalyzer (Bran-Luebbe, TRAACS-800). The NH_4^+ concentration was measured fluorometrically by application of the ortho-phthaldialdehyde (OPA) method (Holmes et al. 1999) using a Turner Design Trilogy fluorometer.

The measurement of $\delta^{15}N$ of NH_4^+ was based on the method by Holmes et al. (1998). In this study, we analyzed the samples that contained over 2 μM NH_4^+ to minimize isotope fractionation due to recovery rate. The filtrate was transferred to incubation bottles, and NaCl, MgO, and an NH_3 trap were added. The NH_3 trap consisted of an acidified 10-mm diameter GF/D filter sandwiched between two 25-mm diameter, 10-μm pore size Teflon membrane filters that floated on the saline samples. Di-ammonium hydrogen citrate was used as the reference for sample correction of isotope deviations due to recovery rate. The samples and references were incubated for 10 to 14 days depending on the incubation bottle sizes such that all NH_4^+ could diffuse out of the solution and be trapped by the filters. During incubation, samples were mixed gently and maintained at 40°C. After incubation, filter packages were removed from the incubation bottles, dried, and stored prior to isotope analysis in a desiccator with sulfuric acid. The $\delta^{15}N$ values were measured using a mass spectrometer (delta S, Finnigan MAT) coupled online via a Conflo-2 interface (Finnigan MAT) with an elemental analyzer (EA1108, Carlo Erba). The recovery of the NH_4^+ retrieval procedure was >80% with a tendency toward better precision at higher concentrations. Measured $\delta^{15}N$ values of samples were corrected by the fractionation of each reference. The reproducibility of the running standard (DL-alanine) was better than ±0.2‰.

The measurement of $\delta^{15}N$ of $NO_3^- + NO_2^-$ was conducted using the denitrifier method (Sigman et al. 2001) with a Thermo Finnigan GasBench and PreCon trace gas concentration system interfaced to a Thermo Scientific Delta V Plus isotope-ratio mass spectrometer at the University of California- Davis Stable Isotope Facility (SIF). Full procedure was done by SIF staff. Except in May 2011, the value of $\delta^{18}O$ of $NO_3^- + NO_2^-$, were measured simultaneously with $\delta^{15}N$ (Casciotti et al. 2002). Because the majority samples included a non-negligible amount of NO_2^- (> 20% of $NO_2^- + NO_3^-$) at offshore sites in July 2011, we show $\delta^{18}O$ data for < 20% of the samples. Hereafter, $NO_3^- + NO_2^-$ is described simply as NO_3^- unless specified otherwise.

POM samples were analyzed for $\delta^{15}N$ and $\delta^{13}C$ values. GF/F filters for this analysis were stored overnight in a desiccator with HCl fumes to remove inorganic carbon. Each dried filter was folded and packed into a tin capsule (Thermo Scientific, 240 06400). The $\delta^{15}N$ and $\delta^{13}C$ values of the POM were measured on a mass spectrometer (Finnigan Mat, delta S) and an elemental analyzer (Carlo Erba, EA1108). Center of Ecological Research-certified reference materials (Tayasu et al. 2011) were used for calibration and verification processes. The reproducibilities of $\delta^{15}N$ and $\delta^{13}C$ were better than ±0.3 and ±0.2‰, respectively. All isotope data are reported in conventional delta notation and are relative to atmospheric N_2 and VPDB standard.

2.3. Mixing model

As a conservative parameter, salinity is commonly used in estuarine studies to derive sources and sinks of nutrients deviating from conservative mixing (Middelburg and Nieuwenhuize 2001; Kasai et al. 2010). When the estuarine nutrient concentration is determined simply by the conservative mixing of river water and seawater nutrients, the concentration of nutrients in estuarine waters (N_{MIX}) depends linearly on salinity:

$$N_{\mathrm{MIX}} = \frac{(S_{\mathrm{s}} \times N_{\mathrm{m}}) + \left((S_{\mathrm{m}} - S_{\mathrm{s}}) \times N_{\mathrm{r}}\right)}{S_{\mathrm{m}}}, \qquad (1)$$

in which s denotes the sampling point, m the marine endmember, r the river endmember, *S* the salinity and *N* the concentrations of the nutrients (NO_3^-, NH_4^+ and PO_4^{3-}). The salinity of the river endmember is zero. Similarly, $\delta^{15}N$ of DIN is expressed as follows:

$$\delta N_{\mathrm{MIX}} = \frac{S_{\mathrm{s}} \times N_{\mathrm{m}} \times \delta N_{\mathrm{m}} + (S_{\mathrm{m}} - S_{\mathrm{s}}) \times N_{\mathrm{r}} \times \delta N_{\mathrm{r}}}{S_{\mathrm{s}} N_{\mathrm{m}} + (S_{\mathrm{m}} - S_{\mathrm{s}}) \times N_{\mathrm{r}}} \quad , \qquad (2)$$

in which δN denotes the $\delta^{15}N$, and δN_{MIX} is the expected $\delta^{15}N$ from the model as a function of *S*. In this study, we calculated only δN_{MIX} of $\delta^{15}N_{\mathrm{NO3}}$, because it was impossible to characterize the $\delta^{15}N_{\mathrm{NH4}}$ of the riverine endmember due to analytical limitations. Values of marine endmembers were from the bottom water (highest salinity water) at Stn. Y10, whereas those of riverine endmembers were obtained from the monitoring data in each month (Figs. 1 and 2) by MLITT and the literature ($\delta^{15}N_{NO3}$ = 10‰; Wada 2009).

Deviations of each constituent from conservative behavior were calculated on the basis of the expected change in concentration or $\delta^{15}N$ due to the conservative mixing model for concentrations (Eq. 1) or $\delta^{15}N$ (Eq. 2) versus the actual change in concentrations, that is, $\Delta N = N_s - N_{MIX}$ or $\Delta\delta^{15}N = \delta N_s - \delta N_{MIX}$. A positive ΔN corresponds to an increase in analyte concentration (production) compared with the conservative estimate, whereas a negative ΔN corresponds to a decrease in the analyte (consumption) (Roberts et al. 2012). A positive $\Delta\delta^{15}N$ of NO_3^- ($\Delta\delta^{15}N_{NO3}$) suggests an isotope effect due to assimilation and/or denitrification, whereas a negative $\Delta\delta^{15}N_{NO3}$ suggests an isotope effect from, for example, partial nitrification (Dähnke et al. 2008; Wankel et al. 2009; Miyajima et al. 2009; Sugimoto et al. 2014).

2.4. Rayleigh equations

The quantitative relationship between $\delta^{15}N_{NO3}$ and NO_3^- concentrations can be theoretically described by the first-order Rayleigh fractionation model. If phytoplankton take up NO_3^- supplied from the river, $\delta^{15}N_{NO3}$ in the estuary can follow the theoretical relationship between $\delta^{15}N_{NO3}$ and NO_3^- concentrations with some isotopic discrimination as expressed by the following equation (Altabet and Francois 2001; Sugimoto et al. 2009b):

$$\delta^{15}\mathrm{N}_{\mathrm{NO3\_ass}} = \delta^{15}\mathrm{N}_{\mathrm{NO3\_ini}} + \varepsilon_{\mathrm{NO3}} \times \ln f_{NO3} \quad , \qquad (3)$$

in which $\delta^{15}N_{NO3\_ass}$ is the $\delta^{15}N_{NO3}$ expected by NO_3^- assimilation, $\delta^{15}N_{NO3\_ini}$ is the $\delta^{15}N$ of the supplied NO_3^-, ε_{NO3} is the isotope discrimination of NO_3^- assimilation by phytoplankton and f_{NO3} ($[NO_3^-]_s/[NO_3^-]_{ini}$) is the residual fraction of NO_3^- utilized by phytoplankton. The values of $[NO_3^-]_s$ and $[NO_3^-]_{ini}$ denote the measured and the initial NO_3^- concentrations of the source, respectively.

On the other hand, $\delta^{15}N_{NO3}$ regenerated by nitrification ($\delta^{15}N_{NO3\_nit}$) can be simulated as follows (Southwell et al. 2008; Sugimoto et al. 2008):

$$\delta^{15}\mathrm{N}_{\mathrm{NO3\_nit}} = \delta^{15}\mathrm{N}_{\mathrm{NH4\_ini}} - \varepsilon_{\mathrm{nit}} \times f_{\mathrm{NH4}} \times \ln f_{\mathrm{NH4}}/(1 - f_{\mathrm{NH4}}) \quad , \qquad (4)$$

in which ε_{nit} is the apparent isotopic discrimination for nitrification in ‰ units and f_{NH4} ($[NH_4^+]_s/[DIN]_s$) is the proportion of NH_4^+ remaining in the water. $[NH_4^+]_s$ and $[DIN]_s$ denote the measured NH_4^+ and DIN concentrations.

Eqs. (3) and (4) assume a closed system (i.e., neither new NO_3^- nor regenerated NH_4^+ is supplied continuously). However, the substrate NO_3^- for assimilation or NH_4^+ for nitrification may be supplied continuously from the upper site or from sufficient organic materials in the estuary, respectively, which conflict with the assumption of the closed system model. Therefore, it is important to assume that the theoretical changes in an open system at a steady state are as follows (Southwell et al. 2008; Sugimoto et al. 2009a):

$$\delta^{15}\mathrm{N}_{\mathrm{NO3\_ass}} = \delta^{15}\mathrm{N}_{\mathrm{NO3\_ini}} - \varepsilon_{\mathrm{NO3}} \times \ln(1 - f_{NO3}) \quad , \qquad (5)$$

$$\delta^{15}\mathrm{N}_{\mathrm{NO3\_nit}} = \delta^{15}\mathrm{N}_{\mathrm{NH4\_ini}} + \varepsilon_{\mathrm{nit}} \times f_{\mathrm{NH4}} \quad . \qquad (6)$$

In reality, the reaction probably represents and an intermediate between these two extreme situations, but we can constrain the results by considering both models.

3. Results

3.1. Physical and biogeochemical properties on each sampling date

Our snapshot sampling for physical and biogeochemical parameters within the estuaries found marked differences among sampling dates, especially in spring 2010 and 2011 (Fig. 3). In May 2010, saltwater showed extensive intrusion into the estuary compared to May 2011 (Fig. 3B). DO concentrations were significantly lower in 2010, with a minimum of 49% (4.1 mg L^{-1}), than those in 2011 (Fig. 3C). Although NO_3^- concentrations were not significantly different between the two years, $\delta^{15}N_{NO3}$ values in 2010 were significantly lower than those in 2011 (Fig. 3E, I, Tables 1, 2). $\delta^{15}N_{NO3}$ in the bottom water at Stn. Y9 showed minimum value (0.1‰, Table 1). The concentrations of NH_4^+ and PO_4^{3-} in 2010 were significantly higher than those in 2011 (Fig. 3F, G), while the ratios of DIN to PO_4^{3-} (N/P) were significantly low in 2010 (Fig. 3H).

In July 2011, saltwater did not show extensive intrusion (Fig. 3B). Water temperature, Chl-a concentrations and $\delta^{15}N_{PN}$ values showed highest values between sampling dates (Fig. 3A, D, L, Table 3). The DO values showed widest range from 15% (1.2 mg L^{-1}) in the bottom layer to 129% (9.1 mg L^{-1}) in the surface layer (Fig. 3C). PO_4^{3-} concentrations significantly increased from spring to summer, while N/P ratio decreased to around Redfield ratio of 16 (Fig. 3G, H).

Saltwater occupied the majority of the estuary in November 2011 (Fig. 3B), since the proportion of freshwater were lowest between sampling dates. The values of DO, Chl-a, $\delta^{15}N_{NO3}$ and $\delta^{15}N_{PN}$ significantly decreased from summer to fall (Fig. 3C, D, I, K), although PO_4^{3-} concentrations and N/P ratios showed higher and lower values as well as in summer, respectively (Fig. 3G, H).

In the coldest water (< 10ºC) period in February 2012, DO concentrations showed near saturated values (Fig. 3A, C). Saltwater intruded extensively into the estuary, but freshwater occupied upper layer (Fig. 3B). From fall to winter, PO_4^{3-} concentrations and N/P ratio significantly decreased and increased, respectively (Fig. 3G, H).

There was no significant difference in $\delta^{15}N_{NH4}$ values on each sampling date, but $\delta^{15}N_{NH4}$

were always higher than $\delta^{15}N_{NO3}$. The C/N ratios of bulk POM during all months showed similar values from 5 to 10, which are similar to those of phytoplankton (6.6; Redfield et al. 1963).

3.2. Concentrations and isotope ratios along the salinity gradient

The concentrations of NO_3^- and NH_4^+ in May 2010 showed conservative or slightly higher values than the mixing line, whereas $\delta^{15}N_{NO3}$ showed lower values (Fig. 4). The mean values of ΔNO_3^-, ΔNH_4^+ and ΔPO_4^{3-} in May 2010 were averaged to near zero, although the $\Delta\delta^{15}N_{NO3}$ in May 2010 showed a mean negative value (Table 6), indicating an importance of productive processes on average across the transect. Contrastingly, net consumptive processes dominated in May 2011 (Table 6), producing lower NO_3^-, NH_4^+ and PO_4^{3-} values than predicted by the mixing line. However, this was not uniform across the salinity gradient. NO_3^- concentrations were lower than the mixing line at low salinity water (<10), but shifted to higher concentrations than predicted by the mixing at the high salinity water.

In July 2011, the concentrations of NO_3^- and NH_4^+ in low-salinity waters (< 10) were lower than and similar to the mixing line, respectively, whereas both concentrations in brackish waters (10–25) were higher than the mixing line (Fig. 4). Positive average values of ΔNO_3^-, ΔNH_4^+ and ΔPO_4^{3-} across the transect (Table 6) indicated that net productive process dominated in summer, although non-negligible consumptive process occurred within the estuary. Moving toward the higher salinity area, there was a shift from $\delta^{15}N_{NO3}$ higher than the mixing line to $\delta^{15}N_{NO3}$ lower than the mixing line (Fig. 4). This means that the consumptive process occurred in the lower salinity area, but productive process occurred in the higher salinity area.

In November 2011, NO_3^- concentrations considerably increased from mixing line. High average values of ΔNO_3^-, ΔNH_4^+ and ΔPO_4^{3-} (Table 6) indicated that net productive process dominated within the estuary, although the deviations of $\delta^{15}N_{NO3}$ from the mixing line were slightly positive (Fig. 4). In February 2012, in comparison with the mixing line, mean ΔNO_3^- showed highest values with higher values, whereas mean ΔPO_4^{3-} was zero (Table 6). The $\delta^{15}N_{NO3}$ values showed conservative mixing, and the ranges of $\Delta\delta^{15}N_{NO3}$ were the smallest during all months (Fig. 4 and Table 6).

3.3 Relationships among isotope ratios, nitrogen concentrations and DO

When the NO_3^- concentrations were higher than ~40 μM, $\delta^{15}N_{NO3}$ and $\delta^{18}O_{NO3}$ showed relatively constant values around 8–12‰ and 0–4‰, respectively (Fig. 5), indicating isotope ratios of riverine NO_3^- have almost constant values regardless of the season. With the lower NO_3^- concentrations (<~40 μM), however, $\delta^{15}N_{NO3}$ values showed two contrasting trends. In May 2011 and February 2012, $\delta^{15}N_{NO3}$ values slightly increased with a decrease in NO_3^- concentrations, whereas $\delta^{15}N_{NO3}$ values considerably decreased with the NO_3^- concentration in May 2010 and November 2011. The values of $\delta^{15}N_{NO3}$ in July 2011 showed both trends: an increase until ~20 μM but a decrease from ~20 μM with a decrease in NO_3^- concentrations. $\delta^{15}N_{NO3}$ and $\delta^{18}O_{NO3}$ showed higher values in near-saturated DO conditions (> 80%), and the lowest $\delta^{15}N_{NO3}$ and $\delta^{18}O_{NO3}$ values were observed when the DO concentration was 40–80% and <80%, respectively. On the other hand, $\delta^{15}N_{NH4}$ values converged to around 12 to 18‰ which corresponded to waters with low DO (< 80%), where they showed low values with < 5 μM of NH_4^+ and > 80% of DO.

4. Discussion

4.1. Significance of internal biogeochemical processes within the estuary

We found that, regardless of the season of sampling, the mean ΔDIN and ΔPO_4^{3-} values were mostly positive and/or conservative, except in May 2011 (Table 6). This indicates that on average across the transect net productive process dominated within the estuary. Nutrient supply from remineralization would play a prominent role in sources in most months, particularly in summer and autumn, since direct nutrient supply from external sources such as groundwater is minor component in this region (Yasumoto et al. 2010). However, this was not uniform across the salinity gradient. For example, in July 2011, nutrient concentrations tended to be lower than predicted by the mixing in the lower salinity water, but shifted to concentrations higher than predicted by the mixing in the higher salinity water (Fig. 4). Similarly, $\delta^{15}N_{NO3}$ showed higher values than predicted by the mixing line in the lower salinity water, but decreased to $\delta^{15}N_{NO3}$ lower than predicted by the mixing line in the higher salinity water. These results indicate a change in dominant process from consumption to production moving toward the higher salinity area.

Positive and negative deviations in the $\delta^{15}N$ of NO_3^-, which is the major form of DIN, showed the importance of internal biogeochemical processes (Fig. 4 and Table 6). The negative relationship between $\delta^{15}N_{NO3}$ and NO_3^- concentrations manifests as both spatial and temporal phenomena of NO_3^- assimilation by phytoplankton (Altabet and Francois 2001; Sugimoto et al. 2009b). In contrast, a positive exponential relationship between $\delta^{15}N_{NO3}$ and NO_3^- concentrations was obtained when nitrification was dominant in nitrogen cycle (Sugimoto et al., 2009a). Both relationships were clearly found below 40 μM NO_3^- (Fig. 5), and thus the isotope effects of NO_3^- assimilation and/or nitrification likely causes spatial and temporal variations in $\delta^{15}N_{NO3}$.

4.2. Evaluation of NO_3^- assimilation and nitrification within the estuary

Quantitative influence of NO_3^- assimilation and nitrification on DIN dynamics can be evaluated using Rayleigh equations. To calculate Eqs. (3) and (5), we assumed $\delta^{15}N_{NO3\_ini} = 10‰$, because $\delta^{15}N_{NO3}$ values converged to approximately 10‰ above 40 μM NO_3^- (Fig. 5), and this value is similar to the $\delta^{15}N_{NO3}$ value of the freshwater source in the Yodo River (9.6 to 10.5‰; Wada 2009). The values of $[NO_3^-]_{ini}$ were from the monitoring data in each month (Fig. 2). As a result, in the case of NO_3^- assimilation (Fig. 6A), most $\delta^{15}N_{NO3}$ values in May 2011, July 2011, and February 2012 plotted within the range of -1 to -7‰ of ε_{ass}, which is similar to previously reported values from field studies (Horrigan et al. 1990; Lehmann et al. 2004).

On the other hand, to calculate Eqs. (4) and (6), we have used 12‰ as $\delta^{15}N_{NH4\_ini}$. This value was estimated from the minimum case of $\delta^{15}N_{NH4}$ convergence value in low DO waters (12 to 18‰, Fig. 5). In Ise Bay, negative $\delta^{15}N_{NO3}$ values caused by nitrification were observed in slightly depleted DO waters (approximately 2.6–6.4 mg L^{-1}) in spring (Sugimoto et al. 2009a). Similar DO values (40–80% = 2.5–7 mg L^{-1}, Fig. 5) suggest the dominant influence of DIN remineralization and subsequent nitrification. In May 2010, most $\delta^{15}N_{NO3}$ values were plotted within the ε_{nit} range of -15 to -25‰ of the both models (Fig. 6B), but $\delta^{15}N_{NO3}$ values in November 2011 could be explained by the steady-state model of Eq. (6) with -15 to -25‰ of ε_{nit}. These results may be supported by $\delta^{18}O_{NO3}$ reflecting the $\delta^{18}O$ of ambient water ($\delta^{18}O_{H2O}$), because it is directly sensitive to that degree of nitrification (Casciotti et al. 2002). If we assume that the $\delta^{18}O_{NO3}$ produced by nitrification is slightly higher than that of ambient estuarine water ($\delta^{18}O_{H2O}$ = -7 to 0‰, Nishida et al. 2011), the $\delta^{18}O_{NO3}$ would tend to have relatively negative values near 0‰. The $\delta^{18}O_{NO3}$ could also be affected by the $\delta^{18}O$ of dissolved O_2 in low DO water, in which O_2 has high $\delta^{18}O$ due to respiration (Quay et al. 1995). However, no increasing trends of $\delta^{18}O_{NO3}$ below 80% DO (Fig. 5) indicate the non-negligible effect of dissolved O_2 incorporation.

4.3. Co-occurrence of DIN assimilation and nitrification

The mean ΔNO_3^- in July 2011 was significantly lower than that in November 2011, although the mean values of ΔNH_4^+ and ΔPO_4^{3-} in both months showed similar positive values (Table 6). The $\Delta\delta^{15}N_{NO3}$ values showed positive linear relationships with DO% ($r^2 = 0.88$, $p < 0.01$) and Chl-*a* concentrations ($r^2 = 0.63$, $p < 0.01$) in July, indicating co-occurrence of NO_3^-

regeneration (nitrification) and NO_3^- assimilation within the estuary. These findings indicate that NO_3^- assimilation by phytoplankton blooming is likely to inhibit the accumulation of NO_3^-. These results were supported by a slope of 1.1 of $\delta^{15}N_{NO3}$ vs $\delta^{18}O_{NO3}$ in July 2011 ($r^2 = 0.49$, $p < 0.01$), because NO_3^- assimilation leads to an enrichment of $\delta^{15}N_{NO3}$ and $\delta^{18}O_{NO3}$ on a slope of 1 to 1 (Granger et al. 2004). The contribution rates of NO_3^- assimilation on $\delta^{15}N_{NO3}$ signatures (f_{ass}) can be expressed simply as:

$$f_{ass} = 100 \times \frac{\delta^{15}N_{\mathrm{NO3\_S}} - \delta^{15}N_{NO3_{nit}}}{\delta^{15}N_{NO3_{ass}} - \delta^{15}N_{NO3_{nit}}} \quad , \qquad (7)$$

in which $\delta^{15}N_{NO3\_S}$ is the observed isotopic value. If f_{ass} shows unreasonable estimates (i.e., >100% or negative values), we assumed it to be 100% or 0%. Using equations (3), (4), (5), and (6), contribution rates were estimated as 72±26% (mean±SD) with changing values of ε_{nit} (-15 to -25‰) and ε_{ass} (-4 to -7‰), although f_{ass} decreased moving toward the ocean (Fig. 7). These results suggest that NO_3^- assimilation by phytoplankton contributed to drawdown of NO_3^- and limited its accumulation in the estuary.

However, if NO_3^- assimilation is the major regulator of the $\delta^{15}N$ values in phytoplankton, its $\delta^{15}N$ should be equal to or less than that of NO_3^-. The observed $\delta^{15}N$ differences between PN and NO_3^- in July 2011 ranged from -1.0 to 14.5‰, with a mean ± SD value of 6.6 ± 4.4‰, which was significantly higher than those during the other months (Fig. 8). The positive differences in July 2011, when Chl-a concentrations were significantly high, are explained only by the assimilation of ^{15}N-enriched NH_4^+ (Fig. 3 and Table 3). Because an assimilation of NH_4^+ by phytoplankton disturbs the oxidation of NH_4^+ to NO_3^- via NO_2^-, competition for NH_4^+ uptake by phytoplankton and NH_4^+ oxidizing bacteria would explain the limited increase in NO_3^- concentrations.

Sufficient concentrations of NH_4^+ (> 1 μM, Figs. 3 and 4) for phytoplankton demand would inhibit the assimilation of NO_3^-, since phytoplankton uptake NH_4^+ preferentially than NO_3^- (Dortch 1990; Pennock et al. 1987; York et al. 2007). The %NH_4^+ utilization (uNH_4) during phytoplankton blooming in July 2011 could be determined by applying the following equation (York et al. 2007),

$$\mathrm{uNH_4} = 100 \times \frac{[(\delta^{15}\mathrm{N_{NO3}} - \varepsilon_{\mathrm{NO3}}) - \delta^{15}\mathrm{N_{PHY}}]}{(\delta^{15}\mathrm{N_{NO3}} - \varepsilon_{\mathrm{NO3}}) - (\delta^{15}\mathrm{N_{NH4}} - \varepsilon_{\mathrm{NH4}})} \quad , \qquad (8)$$

In which the $\delta^{15}N_{PHY}$ is the $\delta^{15}N$ value of phytoplankton. In this study, we assumed $\delta^{15}N_{PN}$ as $\delta^{15}N_{PHY}$, because low C/N ratios showed the dominance of phytoplankton (Fig. 3). The fractionation factors for NH_4^+ assimilation and NO_3^- assimilation are ε_{NH4} and ε_{NO3}, respectively. The factor ε_{NO3} had values of -4‰ and -7‰, which were obtained from the Rayleigh fractionation model in Fig. 6. The value of ε_{NH4} may be determined by applying the following empirical equation (Liu et al. 2013):

$$\varepsilon_{\mathrm{NH4}} = -39 \exp \frac{-0.0025\mathrm{C}}{1 + 55/\mathrm{C}} - 2[1 - \exp(-0.0025\mathrm{C})] \quad , \qquad (9)$$

in which C is the NH_4^+ concentration (μM). In this case, ε_{NH4} varied from -9.7 to -1.4‰. If uNH_4 shows unreasonable estimates (i.e., >100% or negative values), we assume it to be 100% or 0%. As a result, we found that phytoplankton assimilated from 43.8 to 44.7% on average, of their N as NH_4^+. These results imply that co-assimilation of NH_4^+ and NO_3^- by phytoplankton inhibited NO_3^- accumulation in July 2011.

5. Conclusions

Although delivery of riverine DIN, which is mainly composed of NO_3^-, into the Yodo River estuary is usually dominated largely by seawater mixing, internal biogeochemical processes of DIN assimilation by phytoplankton and DIN production by remineralization and subsequent nitrification within the estuary offer the most reasonable explanations for the observed deviations in NO_3^- isotopic compositions from mixing behavior. Co-assimilation of regenerated NH_4^+ within the estuary and riverine NO_3^- as well as co-occurrence of DIN assimilation and regeneration complicate nutrient dynamics. However, we found that, regardless of the season, the estuarine mixing behavior is mostly conservative or productive. A significant net source of DIN as well as DIP is present within the Yodo River estuary. These results suggest that recycled nutrients within the estuary could have a non-negligible impact on eutrophication in Osaka Bay, despite the general belief that riverine nitrogen loadings from the land are major trigger of eutrophication in the bay (Yasuhara et al. 2007; Nakatani et al. 2011).

Acknowledgments

We are grateful to three anonymous reviewers for their helpful comments and suggestions. Isotope analysis was conducted using Cooperative Research Facilities (Isotope Ratio Mass Spectrometer) of Center for Ecological Research, Kyoto University. This work was supported by JSPS KAKENHI Grant Number 24658175.

References

Altabet MA, Francois R (2001) Nitrogen isotope biogeochemistry of the Antarctic Polar Frontal Zone at 170°W. Deep-Sea Res 48: 4247–4273.

Bonaglia S, Deutsch B, Bartoli M, Marchant HK, Brüchert V (2014) Seasonal oxygen, nitrogen and phosphorous benthic cycling along an impacted Baltic Sea estuary: regulation and spatial patterns. Biogeochemistry 119: 139-160.

Brion N, Baeyens W, De Galan S, Elskens M, Laane RW (2004) The North Sea: source or sink for nitrogen and phosphorus to the Atlantic Ocean? Biogeochemistry 68: 277-296.

Casciotti KL, Sigman DM, Galanter Hastings M, Böhlke JK, Hilkert A (2002) Measurement of the oxygen isotopic composition of nitrate in seawater and freshwater using the denitrifier method. Anal Chem 74: 4905 -4912.

Dähnke K, Bahlmann E, Emeis K (2008) A nitrate sink in estuaries? An assessment by means of stable nitrate isotopes in the Elbe estuary. Limnol Oceanogr 53: 1504-1511.

Dortch Q (1990) The interaction between ammonium and nitrate uptake in phytoplankton. Mar Ecol Prog Ser 61: 183-201.

Eyre BD (2000) Regional evaluation of nutrient transformation and phytoplankton growth in nine river-dominated sub-tropical east Australian estuaries. Mar Ecol Prog Ser 205: 61-83.

Giblin AE, Weston NB, Banta GT, Tucker J, Hopkinson CS (2010) The effects of salinity on nitrogen losses from an oligohaline estuarine sediment. Estuar Coast 33(5): 1054-1068.

Granger J, Sigman DM, Needoba JA, Harrison PJ (2004) Coupled nitrogen and oxygen isotope fractionation of nitrate during assimilation by cultures of marine phytoplankton. Limnol Oceanogr 49: 1763-1773.

Hayashi M, Yanagi T (2008) Analysis of change of red tide species in Yodo River estuary by the numerical ecosystem model. Mar Poll Bull 57: 103-107.

Holmes RM, Aminot A, Kérouel R, Hooker BA, Peterson BJ (1999) A simple and precise method for measuring ammonium in marine and freshwater ecosystems. Can J Fish Aquat Sci 56: 1801-1808.

Holmes RM, McClelland JW, Sigman DM, Fry B, Peterson BJ (1998) Measuring ^{15}N-NH_4^+ in marine, estuarine and fresh waters: an adaptation of the ammonium diffusion methods for samples with low ammonium concentrations. Mar Chem 60: 235-243.

Horrigan SG, Montoya JP, Nevins JL, McCarthy JJ (1990) Natural isotopic composition of dissolved inorganic nitrogen in the Chesapeake Bay. Estuar Coast Shelf Sci 30: 393–410.

Jickells T, Andrews J, Samways G, Sanders R, Malcolm S, Sivyer D, Parker R, Nedwell D, Trimmer M, Ridgway J (2000) Nutrient fluxes through the Humber estuary-Past, present and future. AMBIO: A Journal of the Human Environment 29: 130-135.

Kasai A, Kurikawa Y, Ueno M, Robert D, Yamashita Y (2010) Salt-wedge intrusion of seawater and its implication for phytoplankton dynamics in the Yura Estuary, Japan. Estuar Coast Shelf Sci 86: 408–414.

Lehmann MF, Bernasconi SM, McKenzie JA, Barbieri A, Simona M, Veronesi M (2004) Seasonal variation of the $\delta^{13}C$ and $\delta^{15}N$ of particulate and dissolved carbon and nitrogen in Lake Lugano: Constraints on biogeochemical cycling in a eutrophic lake. Limnol Oceanogr 49: 415-429.

Liu KK, Kao SJ, Chiang KP, Gong GC, Chang J, Cheng JS, Lan CY (2013) Concentration dependent nitrogen isotope fractionation during ammonium uptake by phytoplankton under an algal bloom condition in the Danshuei estuary, northen Taiwan. Mar Chem 157: 242-252.

Middelburg JJ, Nieuwenhuize J (2001) Nitrogen isotope tracing of dissolved inorganic nitrogen behavior in tidal estuaries. Estuar Coast Shelf Sci 53: 385–391.

Miyajima T, Yoshimizu C, Tsuboi Y, Tanaka Y, Tayasu I, Nagata T, Koike I (2009) Longitudinal distribution of nitrate $\delta^{15}N$ and $\delta^{18}O$ in two contrasting tropical rivers: implications for instream nitrogen cycling. Biogeochemistry 95: 243-260.

Nakajima M, Fujiwara T (2007) Estuarine circulation and hypoxic water mass in Osaka Bay. Bulletin on Coastal Oceanography 44: 157-163. (in Japanse with English abstract)

Nishida S, Sato K, Nakatani Y (2011) Water mass analysis of coastal sea waters in and around

Osaka Bay using stable isotope ratio. Journal of Japan Society of Civil Engineers B2, 67: 866-870.(in Japanese with English abstract)

Nakatani Y, Kawasumi R, Nishida S (2011) Change of inflow load and water environment in Osaka Bay. Journal of Japan Society of Civil Engineers B2, 67: 886-890. (in Japanese with English abstract)

Pennock JR (1987) Temporal and spatial variability in phytoplankton ammonium and nitrate uptake in the Delaware estuary. Estuar Coast Shelf Sci 24: 841-857.

Quay PD, Wilbur DO, Richey JE, Devol AH, Benner R, Forsberg BR (1995) The ^{18}O:^{16}O of dissolved oxygen in rivers and lakes in the Amazon Basin: determining the ratio of respiration to photosynthesis rates in freshwaters. Limnol Oceanogr 40: 718-729.

Ragueneau O, Lancelot C, Egorov V, Vervlimmeren J, Cociasu A, Déliat G, Krastev A, Daoud N, Rousseau V, Popovitchev V, Brion B, Popa L, Cauwet G (2002) Biogeochemical transformations of inorganic nutrients in the mixing zone between the Danube River and the north-western Black Sea. Estuar Coast Shelf Sci 54(3), 321-336.

Redfield AC, Ketchum BH, Richard FA (1963) The influence of organisms on the composition on seawater. pp. 26–77. *In* M. N. Hill [ed.], The sea. Inter Sci. Pub.

Roberts, K.L., V.M. Eate, B.D. Eyre, D.P. Holland, and P.L.M. Cook. 2012. Hypoxic events stimulate nitrogen recycling in a shallow salt-wedge estuary: The Yarra River estuary, Australia. Limnology and Oceanography 57 (5): 1427-1442.

Seitzinger S, Harrison JA, Böhlke JK, Bouwman AF, Lowrance R, Peterson B, Tobias C, Drecht GV (2006) Denitrification across landscapes and waterscapes: a synthesis. Ecol Appl 16: 2064-2090.

Sigman DM, Casciotti KL, Andreani M, Barford C, Galanter M, Böhlke JK (2001) A bacterial method for the nitrogen isotopic analysis of nitrate in seawater and freshwater. Anal Chem 73:

4145–4153.

Southwell MW, Popp BN, Martens CS (2008) Nitrification controls on fluxes and isotopic composition of nitrate from Florida Keys sponges. Mar Chem 108: 96-108.

Sugimoto R, Kasai A, Miyajima T, Fujita K (2008) Nitrogen isotopic discrimination by water column nitrification in a shallow coastal environment. J Oceanogr 64: 39–48.

Sugimoto R, Kasai A, Miyajima T, Fujita K (2009a) Controlling factors of seasonal variation in the nitrogen isotope ratio of nitrate in a eutrophic coastal environment. Estuar Coast Shelf Sci 85: 231–240.

Sugimoto R, Kasai A, Miyajima T, Fujita K (2009b) Transport of oceanic nitrate from the continental shelf to the coastal basin in relation to the path of the Kuroshio. Cont Shelf Res 29: 1678–1688.

Sugimoto R, Kasai A, Miyajima T, Fujita K (2010) Modeling phytoplankton production in Ise Bay, Japan: Use of nitrogen isotopes to identify dissolved inorganic nitrogen sources. Estuar Coast Shelf Sci 86: 450–466.

Sugimoto R, Sato T, Yoshida T, Tominaga O (2014) Using stable nitrogen isotopes to evaluate the relative importance of external and internal nitrogen loadings on phytoplankton production in a shallow eutrophic lake (Lake Mikata, Japan). Limnol Oceanogr 59: 37-47.

Tayasu, I., Hirasawa, R., Ogawa, N. O., Ohkouchi, N., Yamada, K. (2011) New organic reference materials for carbon-and nitrogen-stable isotope ratio measurements provided by Center for Ecological Research, Kyoto University, and Institute of Biogeosciences, Japan Agency for Marine-Earth Science and Technology. Limnology 12: 261-266.

Tobias CR, Cieri M, Peterson BJ, Deegan LA, Vallino J, Hughes J (2003) Processing watershed-derived nitrogen in a well-flushed New England estuary. Limnol Oceanogr 48: 1766-1778.

Tsujimoto, A., Nomura, R., Yasuhara, M., Yamazaki, H., Yoshikawa, S. (2006) Impact of eutrophication on shallow marine benthic foraminifers over the last 150 years in Osaka Bay, Japan. Marine Micropaleontol 60: 258-268.

Thompson PA (1998) Spatial and temporal patterns of factors influencing phytoplankton in a salt wedge estuary, the Swan River, Western Australia. Estuaries 21: 801-817.

Wada E 2009. Hierarchical Watershed Management–Creation of a watershed as a public space-. Kyoto University Press. (in Japanese)

Yamamoto K, Nabeshima Y, Yamaguchi M, Itakura S (2009) Distribution and abundance of resting cysts of the toxic dinoflagellates *Alexandrium tamarense* and *A. catenella* in 2006 and 2007 in Osaka Bay. Bulletin of Japanse Society of Fisheries Oceanography 73: 57-66.

Yamamoto K, Tsujimura H, Nakajima M, Harrison PJ (2013) Flusing rate and salinity may control the blooms of the toxic dinoflagellate *Alexandrium tamarense* in a river/estuary in Osaka Bay, Japan. J Oceanogr 69: 727-736.

Yasuhara M, Yamazaki H, Tsujimoto A, Hirose K (2007) The effect of long-term spatiotemporal variations in urbanization-induced eutrophication on a benthic ecosystem, Osaka Bay, Japan. Limnol Oceanogr 52: 1633-1644.

Yasumoto J, Nakada S, Taniguhi M, Nakaya S, Umezawa Y, Takahasi M, Nakamura S (2010) Simulation of submarine groundwater discharge to Osaka Bay, Japan. Proceedings of 21st Salt Water Intrusion Meeting: 232-235.

York JK, Tomasky G, Valiela I (2007) Stable isotopic detection of ammonium and nitrate assimilation by phytoplankton in the Waquoit Bay estuarine system. Limnol Oceanogr 52: 144-155.

Xue D, Boeckx P, Wang Z (2014) Nitrate sources and dynamics in a salinized river and estuary – a $\delta^{15}N-NO_3^-$ and $\delta^{18}O-NO_3^-$ isotope approach. Biogeosciences 11, 5857-5967.

Figure captions

Figure 1. Map of the study site. Circles are sampling stations and a triangle indicate the monitoring site of water quality by the Ministry of Land, Infrastructure and Transport, Japan.

Figure 2. Monthly variation in nitrogen concentrations and dissolved inorganic nitrogen to phosphorous (DIN/DIP) ratios in the Yodo River. Data were obtained from the monitoring site of water information system of Ministry of Land, Infrastructure and Transport, Japan. Vertical gray lines show the sampling dates of the estuary. Horizontal dashed line shows the Redfield ratio (DIN/DIP = 16).

Figure 3. Box plots of temperature, salinity, DO concentrations, Chl-*a* concentrations, NO_3^- concentrations, NH_4^+ concentrations, PO_4^{3-} concentrations, $\delta^{15}N-NO_3^-$ and $\delta^{15}N-NH_4^+$, DIN to PO_4^{3-} ratio, $\delta^{15}N$-PN, C/N ratio from Stn. Y5 to Stn. Y9 on each observation date (medians; box = 25-75% CI; error bar 5-95% CI; and plots maximum and minimum). ND means no data. Dates with different letters are significantly different (Kruskal-Wallis ANOVA on ranks, $p < 0.05$).

Figure 4. Salinity versus NO_3^- concentrations, NH_4^+ concentrations, $\delta^{15}N-NO_3^-$ and $\delta^{15}N-NH_4^+$ in the Yodo River estuary. Solid and dashed lines are the conservative mixing lines for NH_4^+ and NO_3^-, respectively.

Figure 5. $\delta^{15}N-NO_3^-$, $\delta^{18}O-NO_3^-$ and $\delta^{15}N-NH_4^+$ plotted in relation to each concentration (left panels) and DO saturation (right panels) for all water samples in May 2010, May 2011, July

2011, November 2011 and February 2012.

Figure 6. (A) Relationships between the residual fraction of NO_3^- (= f_{NO3}) and the $\delta^{15}N\text{-}NO_3^-$. Solid curve (closed system model of Eq. (3)) and dashed lines (open system model of Eq. (5)) indicate the theoretical changes in $\delta^{15}N\text{-}NO_3^-$ by NO_3^- assimilation with ε_{NO3} of -1, -4 and -7‰. (B) Relationships between the residual fraction of NH_4^+ (= f_{NH4}) and the $\delta^{15}N\text{-}NO_3^-$. Solid curve (closed system model of Eq. (4)) and dashed lines (open system model of Eq. (5)) indicate the theoretical changes in $\delta^{15}N\text{-}NO_3^-$ by nitrification with ε_{nit} of -15, -20 and -25‰. Different plots indicate different observations; May 2010 (▲), May 2011 (■), July 2011 (○), November 2011 (×) and February 2012 (●).

Figure 7. Salinity versus the contribution rates of NO_3^- assimilation on $\delta^{15}N_{NO3}$ (f_{ass}) in July 2011. Plots and error bars are mean value and SD changing values of ε_{nit} (-15‰ and -25‰) and ε_{ass} (-4‰ and -7‰) for equations (3), (4), (5), and (6).

Figure 8. Relationships between Chl-a concentrations and $\delta^{15}N$ differences between PN and NO_3^- in May 2011 (■), July 2011 (○), November 2011 (×) and February 2012 (●).

Table 1. Results of elemental and isotopic analyses on 30 May 2010. The depth in parentheses indicates the water depth.

Station	Layer (m)	$NO_3^- + NO_2^-$ (μM)	NH_4^+ (μM)	PO_4^{3-} (μM)	$\delta^{15}N_{NO3}$ (‰)	$\delta^{18}O_{NO3}$ (‰)	$\delta^{15}N_{NH4}$ (‰)	$\delta^{15}N_{PN}$ (‰)	$\delta^{13}C_{POC}$ (‰)	C/N (mol/mol)	Chl-a (μg/L)
Y5	0	58.8	4.7	1.3	8.6	-	-	-	-	-	2.0
	1.5	19.8	12.3	1.6	6.2	-	-	-	-	-	8.0
	2.5 (2.8)	15.2	13.1	1.7	4.7	-	-	-	-	-	18.9
Y6	0	60.2	6.2	1.5	3.6	-	-	-	-	-	1.8
	1.5	16.4	6.7	1.1	5.3	-	-	-	-	-	16.2
	2.7 (3.0)	10.8	6.3	1.5	3.1	-	-	-	-	-	14.1
Y7	0	58.1	6.7	1.6	8.0	-	-	-	-	-	2.5
	1.5	8.3	5.7	1.1	3.0	-	-	-	-	-	12.4
	2.7 (3.0)	6.1	7.2	1.2	1.7	-	-	-	-	-	10.0
Y8	0	44.3	5.5	1.3	8.1	-	-	-	-	-	2.4
	2.0	5.5	2.2	0.7	3.0	-	-	-	-	-	11.4
	3.0	5.3	3.3	0.7	4.2	-	-	-	-	-	7.9
	3.2 (3.5)	6.3	3.1	0.7	3.6	-	-	-	-	-	13.7
Y9	0	56.9	7.1	1.6	6.8	-	-	-	-	-	3.6
	3.0	6.7	2.9	0.7	2.2	-	-	-	-	-	7.3
	6.0	5.3	6.9	1.0	2.8	-	-	-	-	-	9.4
	9.0	4.6	10.1	1.2	2.0	-	-	-	-	-	17.2
	10.5 (11.0)	4.3	12.5	1.5	0.1	-	-	-	-	-	17.4
Y10	0	46.6	8.1	1.5	7.3	-	-	-	-	-	3.5
	3.0	7.4	1.3	0.4	3.5	-	-	-	-	-	2.7
	6.0	7.0	4.7	0.7	0.8	-	-	-	-	-	1.8
	10.0	5.1	4.3	0.6	3.4	-	-	-	-	-	1.4
	11.5 (12.0)	4.6	7.1	0.9	0.5	-	-	-	-	-	8.1

Table 2. Results of elemental and isotopic analyses on 17 May 2011. The depth in parentheses indicates the water depth.

Station	Layer (m)	NO_3^- + NO_2^- (μM)	NH_4^+ (μM)	PO_4^{3-} (μM)	$\delta^{15}N_{NO3}$ (‰)	$\delta^{18}O_{NO3}$ (‰)	$\delta^{15}N_{NH4}$ (‰)	$\delta^{15}N_{PN}$ (‰)	$\delta^{13}C_{POC}$ (‰)	C/N (mol/mol)	Chl-a (μg/L)
Y5	0	28.4	0.9	0.4	9.6	4.1	-	7.0	-26.2	7.5	19.1
	1.0	28.1	0.8	0.4	9.5	3.9	-	6.2	-26.5	6.3	19.3
	1.7 (2.0)	27.4	0.8	0.4	9.3	5.0	-	7.3	-26.3	7.7	18.7
Y6	0	27.5	0.9	0.4	9.2	4.3	-	6.5	-26.3	7.5	18.1
	1.0	27.4	1.0	0.4	9.3	4.2	-	7.4	-26.2	7.8	24.5
	2.6 (2.9)	27.5	1.0	0.4	9.3	4.2	-	7.4	-26.4	8.6	19.2
Y7	0	21.8	1.1	0.4	9.4	3.7	-	7.0	-26.4	7.0	16.1
	1.0	27.7	1.2	0.5	9.1	4.3	-	6.6	-26.2	8.0	18.6
	2.4 (2.7)	27.5	4.8	0.6	9.0	4.8	16.1	6.9	-26.2	8.5	16.2
Y8	0	27.9	1.0	0.4	9.2	4.8	-	7.3	-26.8	6.2	15.9
	2.0	27.8	1.3	0.4	9.1	4.7	-	6.3	-27.3	6.1	15.1
	2.7 (3.0)	22.0	9.3	1.0	9.3	6.1	11.7	6.5	-	6.6	7.6
Y9	0	14.5	1.2	0.2	9.3	2.6	-	6.6	-26.9	5.8	13.1
	3.0	2.9	6.7	0.8	11.6	12.5	20.2	9.9	-24.3	4.8	22.5
	6.0	4.7	6.6	0.7	11.8	24.7	14.6	9.3	-22.8	6.0	1.3
	8.5 (9.0)	2.7	10.7	0.8	10.6	25.8	12.3	8.8	-23.0	6.3	2.2
Y10	0	27.9	4.7	0.3	8.8	4.1	16.4	7.8	-26.4	5.9	11.3
	3.0	11.2	3.9	0.1	11.2	14.3	4.3	10.6	-20.9	5.1	9.8
	6.0	4.6	3.8	0.1	12.4	14.1	12.2	9.7	-21.2	5.8	3.1
	10.0	2.4	4.1	0.3	11.0	7.5	10.5	8.4	-21.7	5.7	1.6
	12.0 (13.5)	1.8	10.7	1.1	6.0	14.7	14.6	7.6	-22.6	7.5	5.9

Table 3. Results of elemental and isotopic analyses on 15 July 2011. The depth in parentheses indicates the water depth, and the $NO_3^- + NO_2^-$ with asterusks indicates the higher NO_2^- fractions (> 20%).

Station	Layer (m)	$NO_3^- + NO_2^-$ (μM)	NH_4^+ (μM)	PO_4^{3-} (μM)	$\delta^{15}N_{NO3}$ (‰)	$\delta^{18}O_{NO3}$ (‰)	$\delta^{15}N_{NH4}$ (‰)	$\delta^{15}N_{PN}$ (‰)	$\delta^{13}C_{POC}$ (‰)	C/N (mol/mol)	Chl-a (μg/L)
Y5	0	33.1	0.8	1.2	12.7	5.0	-	18.3	-28.1	6.1	41.7
	0.5	33.9	1.3	1.4	12.4	4.7	-	16.1	-27.8	8.0	40.8
	1.4 (1.7)	25.2	1.1	1.6	12.7	4.1	-	23.1	-26.8	4.4	41.3
Y6	0	31.9	1.1	1.6	12.3	4.3	-	17.6	-26.2	5.9	55.8
	1	44.2	6.8	3.0	11.2	2.8	20.6	22.9	-24.3	4.5	33.7
	2.8 (3.1)	45.2	15.5	4.2	11.1	1.4	18.0	12.8	-23.3	6.0	36.2
Y7	0	31.5	2.5	1.5	12.6	4.2	3.8	23.1	-24.9	4.7	53.7
	1.5	38.0	13.5	3.6	11.0	2.8	17.3	23.7	-23.0	4.9	47.6
	2.4 (2.7)	26.4	11.8	3.4	10.8	2.8	17.8	18.7	-22.6	6.4	45.7
Y8	0	52.1	5.8	3.4	10.8	2.8	18.2	25.3	-23.8	4.9	35.8
	1	26.2	7.9	1.9	11.6	2.7	14.4	21.0	-22.7	5.5	68.0
	2	32.7	7.8	3.8	11.4	3.4	20.5	12.3	-20.8	6.5	40.1
	3.1 (3.4)	48.1	19.3	3.6	12.8	7.3	15.0	11.7	-24.8	9.2	51.3
Y9	0	83.6	9.5	3.9	12.5	2.3	27.0	19.3	-23.5	5.7	39.1
	3	17.7	10.0	1.9	9.9	2.3	18.3	20.1	-19.5	4.7	29.8
	6	11.9^*	10.3	1.8	8.0	-	17.6	14.5	-19.8	6.8	17.0
	9.5 (10.0)	11.1^*	9.2	2.1	7.3	-	17.4	11.1	-22.9	8.6	14.8
Y10	0	15.1^*	5.1	0.8	16.0	-	13.09	19.1	-19.5	4.9	82.7
	3	3.6^*	2.2	0.1	12.0	-	5.89	11.0	-18.1	6.4	11.5
	6	2.1^*	2.4	0.3	7.6	-	14.45	18.8	-19.1	5.6	21.3
	10	4.5^*	3.7	0.8	3.9	-	12.91	12.9	-18.1	6.4	12.9
	12.0 (12.7)	6.0^*	2.0	0.2	11.2	-	14.85	13.2	-17.9	6.4	38.4

Table 4. Results of elemental and isotopic analyses on 8 November 2011. The depth in parentheses indicates the water depth.

Station	Depth (m)	NO_3^- + NO_2^- (μM)	NH_4^+ (μM)	PO_4^{3-} (μM)	$\delta^{15}N_{NO3}$ (‰)	$\delta^{18}O_{NO3}$ (‰)	$\delta^{15}N_{NH4}$ (‰)	$\delta^{15}N_{PN}$ (‰)	$\delta^{13}C_{POC}$ (‰)	C/N (mol/mol)	Chl-a (μg/L)
Y5	0	37.2	10.6	2.8	10.6	-0.3	20.1	5.5	-25.4	6.2	7.6
	1.0	25.5	12.5	2.9	9.0	-0.4	18.2	5.6	-24.8	6.4	11.8
	1.7 (2.0)	28.3	12.8	3.5	8.8	-0.2	-	5.8	-24.9	7.1	12.8
Y6	0	39.4	10.7	3.0	10.0	-0.5	19.6	5.5	-24.7	5.5	8.0
	1.5	28.2	11.1	3.4	8.4	-0.4	17.8	6.5	-23.9	6.5	10.1
	2.3 (2.6)	21.4	11.0	3.2	7.0	-0.8	17.7	6.0	-24.9	8.4	10.2
Y7	0	42.3	10.0	3.1	8.4	-0.7	17.2	5.3	-25.4	5.6	11.6
	1.5	43.5	10.0	3.3	8.9	-0.7	19.5	5.4	-25.5	5.8	11.9
	2.7 (3.0)	29.8	10.9	3.3	7.5	-1.5	17.5	6.2	-24.5	6.6	9.1
Y8	0	52.1	9.7	3.0	10.9	1.6	19.1	6.2	-24.7	5.6	9.6
	1.0	31.4	6.4	1.9	9.2	-0.8	14.2	7.7	-23.8	6.1	8.4
	2.0	23.3	5.4	2.3	7.7	-0.9	17.6	8.4	-23.6	6.3	7.6
	2.7 (3.0)	41.1	10.0	2.2	9.6	-0.5	14.0	7.2	-24.5	8.6	7.4
Y9	0	54.5	7.6	4.4	10.0	-0.4	17.1	5.2	-24.6	4.9	8.3
	3.0	18.8	1.3	1.1	9.2	-1.5	-	12.8	-20.2	5.7	8.2
	6.0	22.4	1.3	1.4	9.2	-1.5	-	12.8	-20.7	5.3	6.4
	8.5 (9.3)	14.9	3.6	1.3	7.2	-2.9	19.0	10.1	-22.6	7.5	3.3
Y10	0	26.4	5.2	1.1	12.0	1.2	17.7	9.3	-20.8	5.1	4.0
	3.0	16.7	1.6	0.8	9.6	-1.0	-	11.8	-20.7	5.8	4.7
	6.0	16.5	1.1	0.8	9.7	-1.7	-	12.0	-20.5	5.6	4.3
	10.0	12.9	1.9	0.8	7.6	-2.4	-	11.5	-21.0	6.5	2.6
	12.0 (13.1)	8.9	4.1	0.7	6.5	-2.0	15.7	9.9	-21.4	7.4	2.4

Table 5. Results of elemental and isotopic analyses on 21 February 2012. The depth in parentheses indicates the water depth.

Station	Depth (m)	NO_3^- + NO_2^- (μM)	NH_4^+ (μM)	PO_4^{3-} (μM)	$\delta^{15}N_{NO3}$ (‰)	$\delta^{18}O_{NO3}$ (‰)	$\delta^{15}N_{NH4}$ (‰)	$\delta^{15}N_{PN}$ (‰)	$\delta^{13}C_{POC}$ (‰)	C/N (mol/mol)	Chl-a (μg/L)
Y5	0	58.9	3.8	0.6	10.1	0.0	15.3	7.5	-26.0	6.5	11.1
	1.0	55.8	5.1	0.8	9.8	1.3	21.5	7.4	-25.9	6.7	9.8
	2.2 (2.5)	46.4	12.1	1.5	9.6	1.3	16.7	5.8	-23.5	7.4	12.1
Y6	0	59.7	3.7	0.6	9.9	1.1	20.1	6.9	-26.6	6.1	9.9
	1.5	47.6	7.9	1.1	10.0	2.4	17.8	8.4	-24.2	6.8	9.3
	2.7 (3.0)	42.6	8.8	1.2	10.1	2.2	18.2	5.8	-24.9	8.1	12.0
Y7	0	58.3	26.1	0.6	9.9	0.0	18.4	8.7	-26.8	6.4	8.9
	1.5	38.4	5.4	0.7	9.9	1.3	12.1	6.1	-21.9	6.8	16.1
	2.5 (2.8)	18.6	2.6	0.5	11.7	4.5	15.1	7.7	-23.0	7.1	12.2
Y8	0	57.9	5.2	0.8	10.2	0.5	14.3	7.2	-25.8	6.3	7.4
	1.0	37.9	10.3	1.0	10.1	1.4	20.3	7.7	-22.1	6.4	22.6
	2.0	31.6	4.8	0.6	10.0	1.3	18.3	7.9	-22.0	6.5	13.5
	2.8 (3.1)	19.8	3.1	0.4	10.7	2.8	11.1	4.4	-21.1	6.0	10.7
Y9	0	65.2	14.1	1.6	9.8	1.1	20.3	6.6	-25.8	7.2	4.1
	3.0	29.9	5.4	0.6	10.5	2.0	16.4	8.5	-20.5	5.4	22.5
	6.0	15.9	3.0	0.3	12.0	5.4	9.8	10.2	-20.7	5.7	28.0
	9.0 (9.6)	7.3	4.8	0.6	11.2	7.4	14.9	9.8	-21.9	5.8	29.5
Y10	0	84.2	24.4	2.8	10.5	-0.2	15.2	4.2	-25.3	5.9	3.9
	3.0	26.7	6.1	0.5	11.5	5.9	15.7	9.4	-20.5	5.9	27.0
	6.0	7.3	2.4	0.3	14.1	12.5	11.2	10.1	-20.8	5.9	22.4
	10.0	8.4	7.1	0.5	11.4	4.3	12.8	10.2	-20.8	5.7	16.0
	12.0 (13.1)	8.5	5.1	0.5	11.5	9.9	12.3	9.0	-21.3	5.6	20.7

Table 6. Deviations (mean ± SD, range) of NO_3^-, NH_4^+, DIN, PO_4^{3-} and $\delta^{15}N_{NO3}$ from the conservative mixing values.

Date	ΔNO_3^- (μM)	ΔNH_4^+ (μM)	ΔDIN (μM)	ΔPO_4^{3-} (μM)	$\Delta\delta^{15}N\text{-}NO_3^-$ (‰)
30 May 2010	0.9 ± 4.9	-0.2 ± 3.2	0.8 ± 6.0	0.0 ± 0.3	-0.8 ± 1.8
	(-11.4 to 14.3, n = 19)	(-5.7 to 5.4, n = 19)	(-9.3 to 17.3, n = 19)	(-0.5 to 0.6, n = 19)	(-6.3 to 2.1, n = 19)
17 May 2011	-10.4 ± 8.1	-3.0 ± 2.2	-13.3 ± 7.9	-0.5 ± 0.2	0.7 ± 2.0
	(-27.7 to 4.5, n = 19)	(-6.7 to 2.8, n = 19)	(-30.8 to -0.2, n = 19)	(-1.0 to 0.0, n = 19)	(-1.2 to 4.6, n = 16)
15 Jul 2011	1.3 ± 15.0	4.2 ± 4.7	5.5 ± 18.5	1.3 ± 1.2	0.5 ± 3.0
	(-13.5 to 49.5, n = 20)	(-1.3 to 13.4, n = 20)	(-14.5 to 57.0, n = 20)	(-0.3 to 3.5, n = 19)	(-7.1 to 5.9, n = 19)
8 Nov 2011	13.1 ± 8.9	3.3 ± 4.1	16.3 ± 11.0	1.5 ± 1.0	1.1 ± 1.2
	(0.1 to 31.8, n = 21)	(-2.9 to 8.9, n = 21)	(1.0 to 36.9, n = 21)	(0.1 to 3.4, n = 19)	(-0.9 to 3.7, n = 19)
21 Feb 2012	15.7 ± 13.0	1.2 ± 5.9	16.9 ± 16.9	0.0 ± 0.6	-0.1 ± 0.8
	(-2.2 to 55.9, n = 20)	(-6.2 to 17.2, n = 20)	(-5.0 to 73.1, n = 20)	(-0.8 to 1.9, n = 19)	(-1.0 to 2.8, n = 19)

Figure 1 (Sugimoto and Kasai)

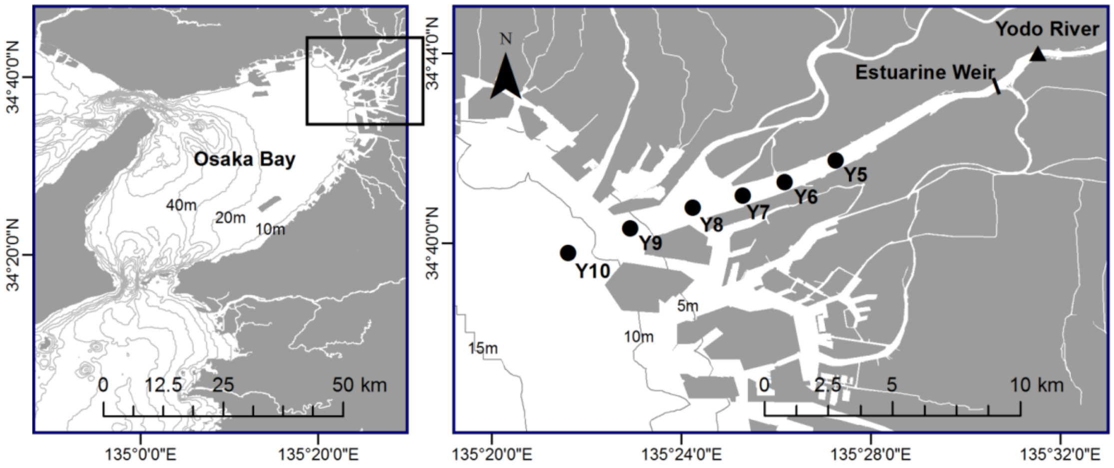

Figure 2 (Sugimoto and Kasai)

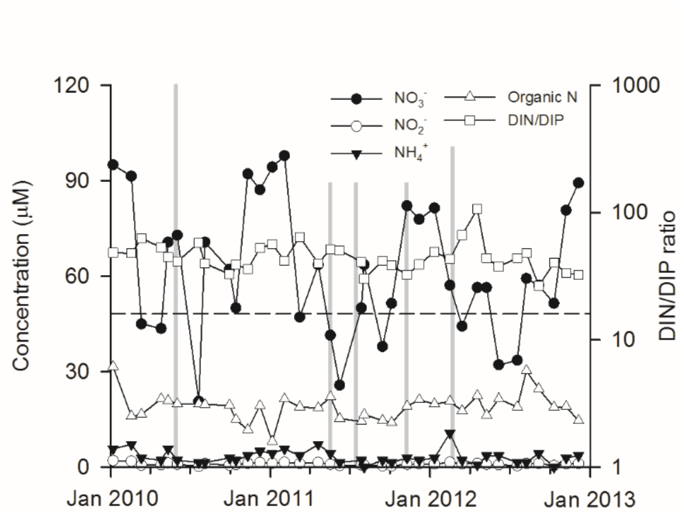

Figure 3 (Sugimoto and Kasai)

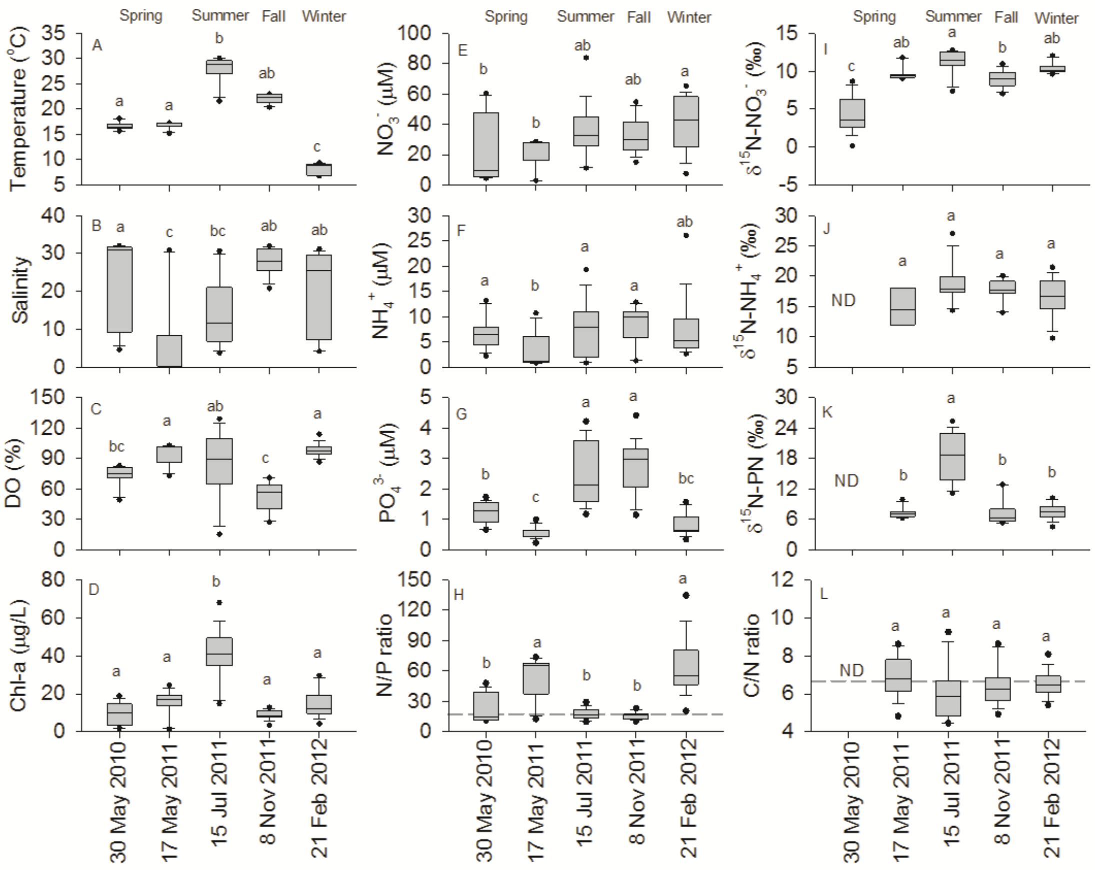

Figure 4 (Sugimoto and Kasai)

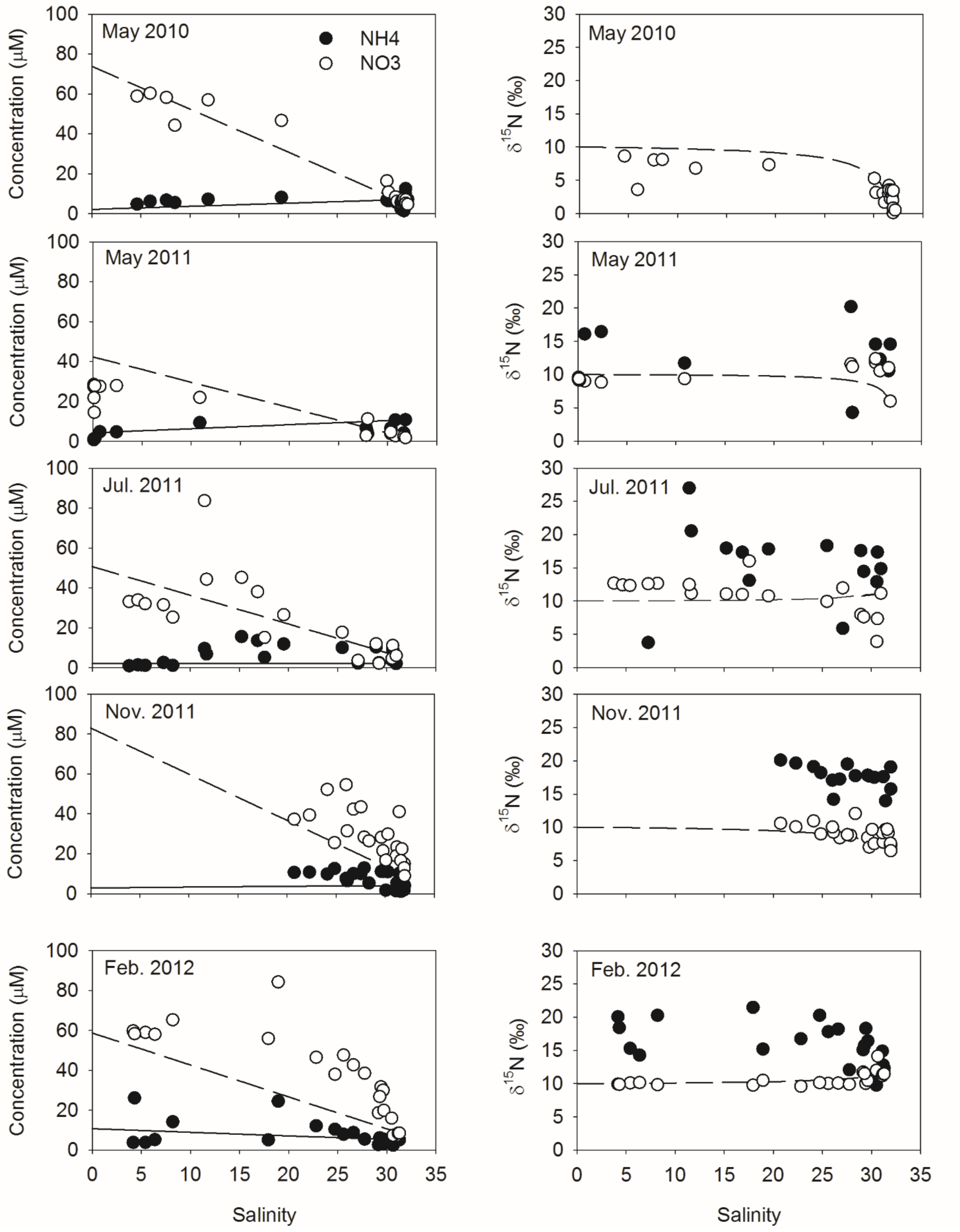

Figure 5 (Sugimoto and Kasai)

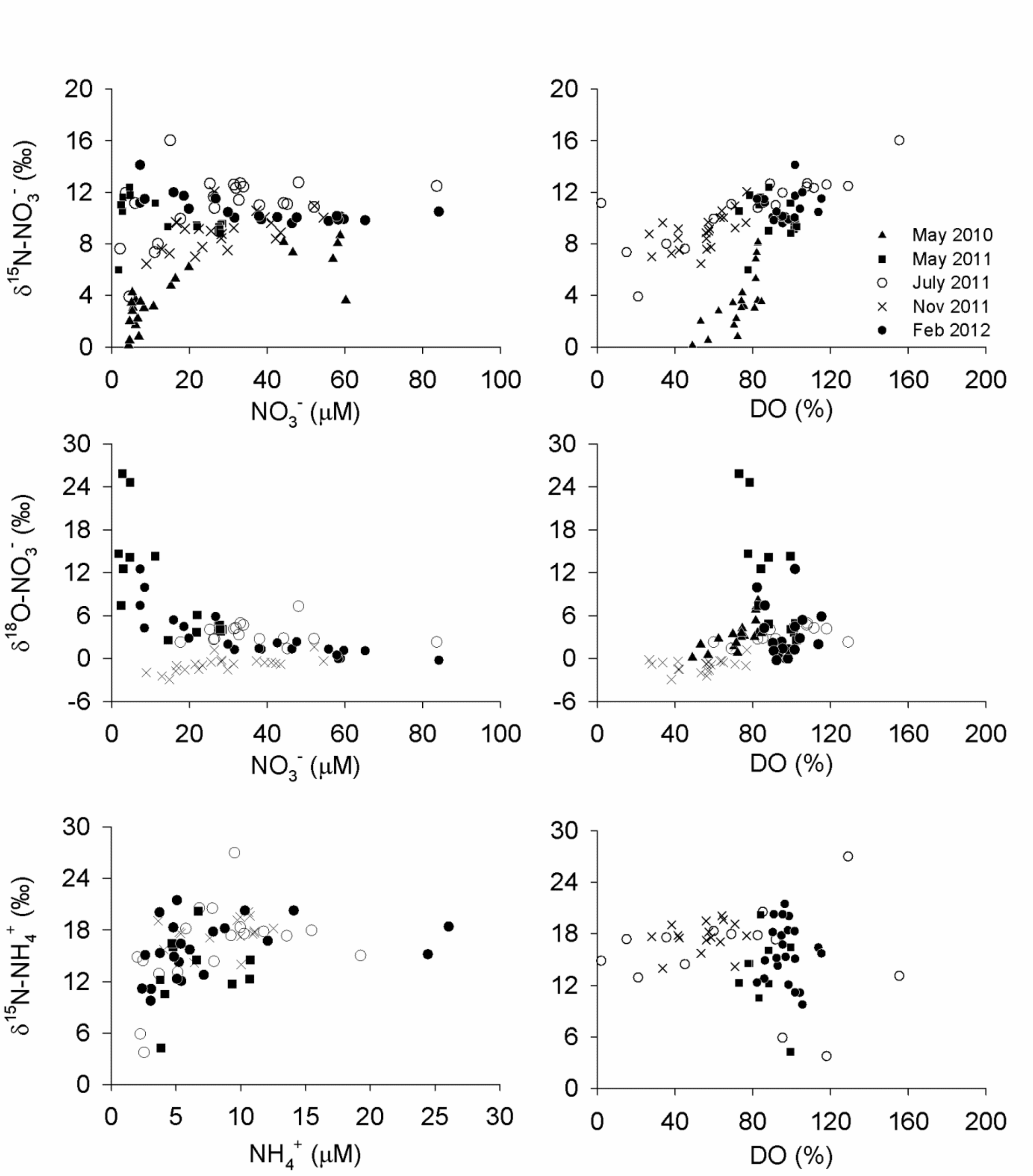

Figure 7 (Sugimoto and Kasai)

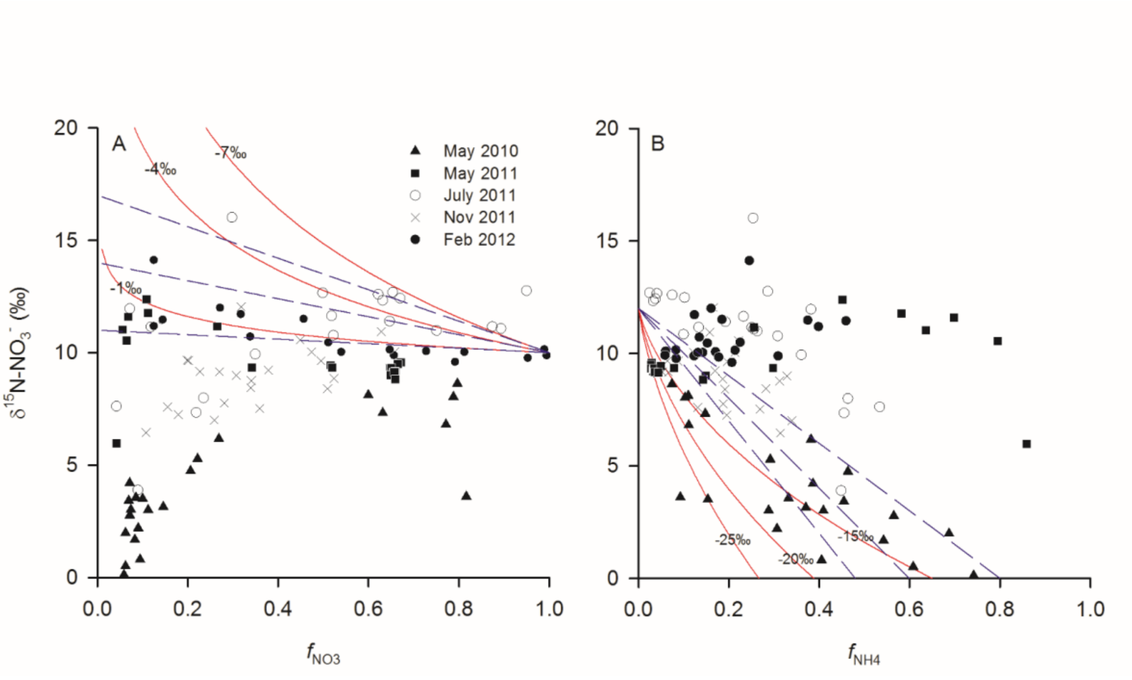

Figure 7 (Sugimoto and Kasai)

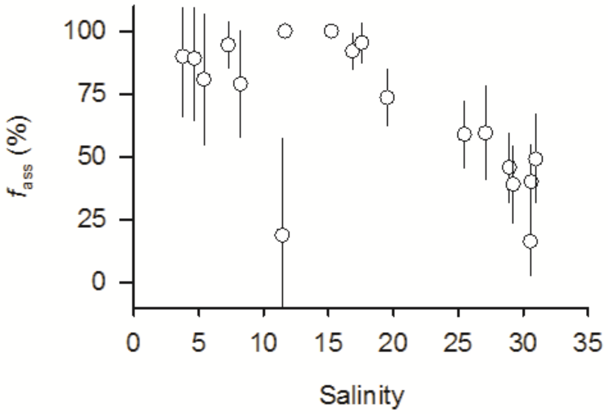

Figure 8 (Sugimoto and Kasai)